Resonance Raman Spectra of Carbon Nanotubes by Cross-Polarized Light

A. Jorio,[1,6] M. A. Pimenta,[1] A. G. Souza Filho,[2,6] Ge. G. Samsonidze,[7] A. K. Swan,[3] M. S. Ünlü,[3] B. B. Goldberg,[3,4] R. Saito,[5] G. Dresselhaus,[8] and M. S. Dresselhaus[6,7]

[1]*Departamento de Física, Universidade Federal de Minas Gerais, Belo Horizonte, MG, 30123-970 Brazil*
[2]*Departamento de Física, Universidade Federal do Ceará, Fortaleza, CE, 60455-760 Brazil*
[3]*Electrical and Computer Engineering Department, Boston University, Boston, Massachusetts 02215*
[4]*Department of Physics, Boston University, Boston, Massachusetts 02215*
[5]*Department of Physics, Tohoku University and CREST JST, Sendai 980, Japan*
[6]*Department of Physics, Massachusetts Institute of Technology, Cambridge, Massachusetts 02139-4307*
[7]*Department of Electrical Engineering and Computer Science, Massachusetts Institute of Technology, Cambridge, Massachusetts 02139-4307*
[8]*Francis Bitter Magnet Laboratory, Massachusetts Institute of Technology, Cambridge, Massachusetts 02139-4307*

(Received 10 August 2002; published 14 March 2003)

Resonance Raman studies on single wall carbon nanotubes (SWNTs) show that resonance with cross polarized light, i.e., with the $E_{\mu,\mu\pm1}$ van Hove singularities in the joint density of states needs to be taken into account when analyzing the Raman and optical absorption spectra from isolated SWNTs. This study is performed by analyzing the polarization, laser energy, and diameter dependence of two Raman features, the tangential modes (G band) and a second-order mode (G' band), at the isolated SWNT level.

DOI: 10.1103/PhysRevLett.90.107403 PACS numbers: 78.30.Na, 63.22.+m, 78.20.Bh, 78.66.Tr

Raman spectroscopy at the single nanotube level has now been achieved by many groups [1–3], and recently optical absorption spectra have also been acquired from isolated single wall carbon nanotubes (SWNTs) [4], thus providing rapid development of this research field. Up to now, it has been well accepted that optical spectra (absorption, resonance Raman scattering, etc.) are dominated by absorption/emission of light polarized parallel to the tube axis, involving transitions between electronic states at van Hove singularities (VHSs) $E^{v}_{i,\mu} \rightarrow E^{c}_{i,\mu}$, where v and c stand for valence and conduction bands, respectively, i is the van Hove singularity index, and μ is the cutting-line index [5]. In other words, only $E_{\mu\mu}$ (that is equivalent to E_{ii}) van Hove singularities in the joint density of states (JDOS) have been taken into account thus far when analyzing Raman and optical absorption spectra from SWNTs [5]. We here show that resonance Raman scattering for cross polarized light involving the $E_{\mu,\mu\pm1}$ VHSs in the JDOS also needs to be taken into account when analyzing Raman spectra from isolated SWNTs. This important result implies that asymmetries between electronic levels above and below the Fermi level in SWNTs (related to the overlap integral parameter s in the tight binding approximation) [5] can be obtained experimentally by studying the JDOS optically. This asymmetry cannot be studied by analyzing $E_{\mu\mu}$ transitions because the effect of unequal spacings between levels in the conduction and valence bands cancel each other in $E_{\mu\mu}$ transitions. However, if $s \neq 0$ the optical transition energies $E_{\mu,\mu\pm1}$ and $E_{\mu\pm1,\mu}$ are no longer equal, and the difference gives rise to valence and conduction band asymmetry.

In this work the Raman spectra from isolated SWNTs on a Si/SiO_2 substrate [2] (less than 1 SWNT/μm^2) were acquired in the back-scattering geometry, under ambient conditions, using standard Raman spectrometers and $E_{\text{laser}} = 1.58$, 1.92, 2.18, 2.41, and 2.54 eV. We performed Raman measurements for five different isolated SWNTs with two different laser lines (2.41 and 2.54 eV) on *the same physical* SWNT to determine whether different Raman bands exhibit frequency dispersion at the single nanotube level. Figure 1 shows the tangential modes (G band at $\sim 1580\ \text{cm}^{-1}$) and a second-order feature (G' band at $\sim 2670\ \text{cm}^{-1}$) in the Raman spectra from two isolated semiconducting SWNTs located at different laser spots on the sample. These are two key Raman features for understanding the resonance nature of Raman scattering in SWNTs, as discussed below. For each SWNT in Fig. 1, Raman spectra from *the same physical* SWNT are taken using $E_{\text{laser}} = 2.41$ and 2.54 eV. We fit the G-band and G' spectral features for each SWNT using a sum of Lorentzians.

The second-order G' band is an interesting feature that appears in the Raman spectra of SWNTs (and other sp^2 carbon materials) through a second-order (double resonance) Raman process, exhibiting an E_{laser} dependent frequency $\omega_{G'}$ [5–7]. From the G' frequency dispersion $\partial\omega_{G'}/\partial E_{\text{laser}}$ for SWNT bundles [5–7] of 106 cm^{-1}/eV, we expect a change of about $\Delta\omega_{G'} = 14\ \text{cm}^{-1}$ for E_{laser} between 2.41 and 2.54 eV, and the G' band intensities do not exhibit a strong dependence on E_{laser}. Values of $\Delta\omega_{G'}$ obtained from each of five different isolated (n, m) SWNTs using spectra as in Fig. 1 yielded different $\Delta\omega_{G'}$, the smallest observed being $\Delta\omega_{G'} = 6\ \text{cm}^{-1}$ and

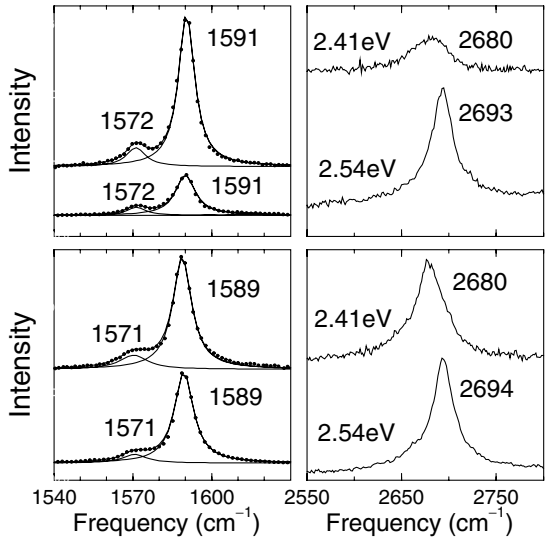

FIG. 1. Raman spectra from two isolated semiconducting SWNTs using $E_{\text{laser}} = 2.41$ eV (top trace) and $E_{\text{laser}} = 2.54$ eV (bottom trace). For each SWNT, ω_{G^-} and ω_{G^+} (left) and $\omega_{G'}$ (right) are in cm^{-1}.

largest $\Delta\omega_{G'} = 18\ \text{cm}^{-1}$. Furthermore, very different $I_{G'}(2.41)/I_{G'}(2.54)$ relative intensities were measured, as shown in Fig. 1. These results clearly show, at the single nanotube level, the rich E_{laser}-dependent behavior of the double resonance process in one-dimensional systems [5–9]. It is interesting to point out that for the five SWNTs the average value is $\Delta\omega_{G'} = 13\ \text{cm}^{-1}$ or $\partial\omega_{G'}/\partial E_{\text{laser}} = 100\ \text{cm}^{-1}/\text{eV}$, which is consistent with the results for SWNT bundles [5–7].

The tangential (G-band) Raman feature appears in SWNT spectra as a complex feature with multiple peaks, in contrast to the single peak ($\omega_{E_{2g}} = 1582\ \text{cm}^{-1}$) found for a 2D graphene sheet [5]. Despite the importance and the large number of prior works devoted to Raman scattering in SWNTs [5], there is still controversy about whether the many peaks within this G band are related to a *single resonance* process and exhibit different symmetries [5,10] or if all belong to a totally symmetric irreducible representation (A symmetry) [1,11] and originate from a *double resonance* Raman scattering process [12]. The G-band resonance Raman spectra in Fig. 1 at two different E_{laser} values differ mostly with regard to total intensity, reflecting how well the resonance condition is obeyed, and no frequency change was observed, despite the 4 cm^{-1} change expected from double resonance theory [12]. Stokes and anti-Stokes measurements also show the same ω_G values for both isolated and bundled SWNTs [9]. This result suggests that the G band is due to a first-order single-resonance process and the multifeatures are related to 1D phonon confinement in SWNTs [5,10].

To discuss the selection rules for the first-order single-resonance Raman scattering process, we consider the most general case, a chiral SWNT (C_N symmetry) [5], with Z as the SWNT axis direction and Y the photon propagation direction. The z basis function belongs to the A irreducible representation, while the x, y basis functions belong to E_1. Thus, using the dipole approximation, the corresponding dipole selection rule for an optical transition between SWNT subbands is given by $E^v_\mu \rightarrow E^c_{\mu'}$ with $(\mu' = \mu)$ for light polarized along Z, and $(\mu' = \mu \pm 1)$ for light polarized along X [13]. For the electron-phonon interaction, phonons can scatter electrons from one cutting line to another, depending on the phonon symmetries. For the Γ-point phonons involved in the G-band scattering, we can define the phonon wave vector $\mathbf{q}$ in an unfolded 2D BZ as $\mathbf{q} = m\mathbf{K}_1$, where $\mathbf{K}_1$ is the separation wave vector between two adjacent cutting lines [5], and m is an integer number indexing the cutting lines. For A phonon mode symmetry, $m = 0$, and for E_j phonon mode symmetries, $m = \pm j$. Note that usually the electron-phonon interaction is a nonresonance process for the intermediate electronic states, since the phonon energies do not match the energy between two electronic subbands. Combining the electron-incident photon, the electron-phonon, and the electron-scattered photon processes in proper sequence yields the following possible Raman processes in SWNTs:

$$E^v_\mu \xrightarrow{\parallel} E^c_\mu \xrightarrow{A(ZZ)} E^c_\mu \xrightarrow{\parallel} E^v_\mu,$$

$$E^v_\mu \xrightarrow{\perp} E^c_{\mu\pm1} \xrightarrow{A(XX)} E^c_{\mu\pm1} \xrightarrow{\perp} E^v_\mu,$$

$$E^v_\mu \xrightarrow{\parallel} E^c_\mu \xrightarrow{E_1(ZX)} E^c_{\mu\pm1} \xrightarrow{\perp} E^v_\mu,$$

$$E^v_\mu \xrightarrow{\perp} E^c_{\mu\pm1} \xrightarrow{E_1(XZ)} E^c_\mu \xrightarrow{\parallel} E^v_\mu,$$

$$E^v_\mu \xrightarrow{\perp} E^c_{\mu\pm1} \xrightarrow{E_2(XX)} E^c_{\mu\mp1} \xrightarrow{\perp} E^v_\mu,$$

consistent with the symmetries for the Raman-active modes $A\,(zz, xx + yy)$, $E_1\,(zx, xz)$, and $E_2\,(xx - yy, xy)$, and with the basis functions for each irreducible representation, given between parentheses. Therefore, considering that the first-order Raman signal from isolated SWNTs can be seen only when in resonance with VHSs, these selection rules imply the following for isolated SWNTs: (1) A modes can be observed for the (ZZ) scattering geometry for resonance with $E_{\mu\mu}$ VHSs, and for the (XX) scattering geometry for resonance with $E_{\mu,\mu\pm1}$ VHSs (the letters between parentheses denote, respectively, the polarization direction for the incident and scattered light); (2) E_1 modes can be observed for the (ZX) scattering geometry for resonance of the incident photon with $E_{\mu\mu}$ VHSs, or for resonance of the scattered photon with $E_{\mu,\mu\pm1}$ VHSs, and for the (XZ) scattering geometry for resonance of the incident photon with $E_{\mu,\mu\pm1}$ VHSs, or for resonance of the scattered photon with $E_{\mu\mu}$ VHSs; (3) E_2 modes can be observed only for

the (XX) scattering geometry for resonance with $E_{\mu,\mu\pm1}$ VHSs. Therefore, depending on the polarization scattering geometry and resonance condition, it is possible to observe 2, 4, or 6 G-band peaks.

Figure 2(a) shows three different G-band Raman spectra from a semiconducting SWNT, but with different directions for the incident light polarization, i.e., θ'_S, $\theta'_S + 40°$, and $\theta'_S + 80°$. We clearly observe well-defined peaks associated with the G-band features, with different relative intensities for the different polarization geometries, and we assign them as follows: 1565 and 1591 $\rightarrow A$; 1572 and 1593 $\rightarrow E_1$; 1554 and 1601 $\rightarrow E_2$. The SWNT in Fig. 2(a) exhibits $\omega_{\mathrm{RBM}} = 180\ \mathrm{cm}^{-1}$ ($d_t = 1.38$ nm) [2]. Spectra from nine other isolated semiconducting SWNTs with similar ω_{RBM} values, i.e., similar diameters, were also found to exhibit different relative intensities for the G-band components, as an indication of the different scattering geometries for the different isolated SWNT measurements.

Figure 2(b) shows two G-band Raman spectra obtained from another semiconducting SWNT ($\omega_{\mathrm{RBM}} = 132\ \mathrm{cm}^{-1}$), with θ''_S and $\theta''_S + 90°$ (see caption to Fig. 2). The spectra can be fit using four sharp Lorentzians, and a broad feature at about 1563 cm^{-1}. This broad feature (FWHM $\sim$50 cm^{-1}) is sometimes observed in weakly resonant G-band spectra from semiconducting SWNTs. A broad feature is also observed at $\sim$1610 cm^{-1} for spectra from other SWNTs. Both broad features may be associated with a double resonance process [12]. From previous polarization Raman studies [10], the sharp peaks at 1554 and 1600 cm^{-1} should be assigned as E_2 modes, while the 1571 and 1591 cm^{-1} peaks should be assigned as unresolved ($A + E_1$) modes, their relative intensities depending on the incident light polarization direction [10]. Of interest is the appearance of such strong E_2 Raman modes under favorable resonance conditions. It is important to stress that the clear observation of E_2 modes at the single nanotube level cannot be explained by the double resonance theory where all modes are assumed to exhibit A symmetry [12].

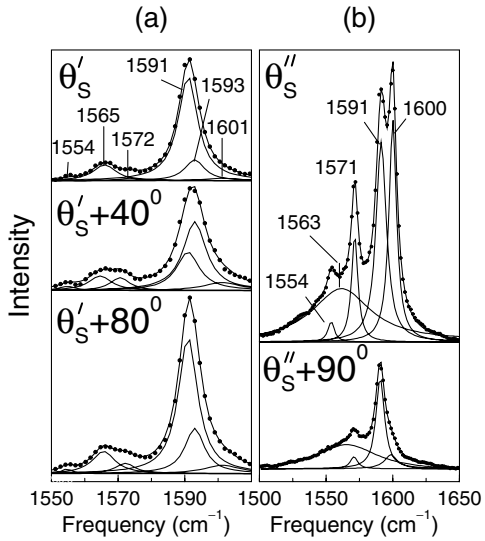

FIG. 2. Polarization scattering geometry dependence for G band from two (a) and (b) isolated SWNTs in resonance with $E_{\mathrm{laser}} = 2.41$ eV. The Lorentzian peak frequencies are in cm^{-1}. θ'_S and θ''_S are the initial angles between the light polarization and SWNT axis directions, not known *a priori*. From the relative intensities polarization behavior of the G-band modes we conclude that $\theta'_S \sim 0°$ and $\theta''_S \sim 90°$.

It is interesting to note the relatively high intensity (XX) spectra that are observed, indicating resonance with $E_{\mu,\mu\pm1}$. For several measured isolated SWNTs, the Raman intensities do not exhibit substantial reduction for any direction of the incident/scattered light, in contrast to previously published results [1,14], which showed an intensity ratio I_{ZZ}:$I_{XX} \sim$ 1:0. From our discussion, it is clear that the so-called "antenna effect" is observed for samples in resonance with only $E_{\mu\mu}$ electronic transitions, and that is the case in Refs. [1,14]. However, in general, the intensity ratio ZZ:XX can assume values larger and smaller than 1, depending on the resonance condition. Thus, all the present and the previous polarization results (Refs. [1,10,14]) can be understood and are consistent with the selection rules discussed here.

Further confirmation for the G-band mode assignment proposed here comes from comparison of experimental results with *ab initio* calculations [15]. Figure 3 plots the G-band mode frequencies for several semiconducting SWNTs in resonance with the incident laser light vs the observed ω_{RBM} (bottom axis) and inverse nanotube diameter $1/d_t = \omega_{\mathrm{RBM}}/248$ (top axis) [2]. The spectra are usually fit using six peaks, although sometimes we use only four or two (see discussion above). Consider G^- and G^+, the G-band features below and above 1580 cm^{-1}, respectively [16]. The presence of two (A and E_1) modes within the G^- peak is clear for lower diameter tubes [see, for example, Fig. 2(a)]. The presence of two (A and E_1) modes within the G^+ peak is not as clear as in the G^- peak. However, the dip between the G^+ and G^- features usually cannot be well fit with only one Lorentzian for G^+. Furthermore, by using two Lorentzians, the spectra can be fit with linewidths approaching the natural linewidth for G-band modes [17], i.e., $\gamma_G \sim 5\ \mathrm{cm}^{-1}$. The E_2 peaks are usually broader, and their weak intensity and contribution from double resonance effects are likely responsible for their broadening.

The solid symbols connected by solid lines come from *ab initio* calculations by Dubay *et al.* [15]. The different solid symbols indicate the different mode symmetries: $\bullet \rightarrow A$, $\blacktriangle \rightarrow E_1$, $\blacksquare \rightarrow E_2$, in agreement with polarization results (see Fig. 2). The theoretical points were downshifted by about 1% to fit the experimental data (see caption). The observed d_t dependence of the frequencies for each of the three higher frequency G^+-band modes (A, E_1, and E_2) are in very good agreement with theory [15], showing little d_t dependence. For the three lower frequency G^--band modes, both *ab initio* calculations

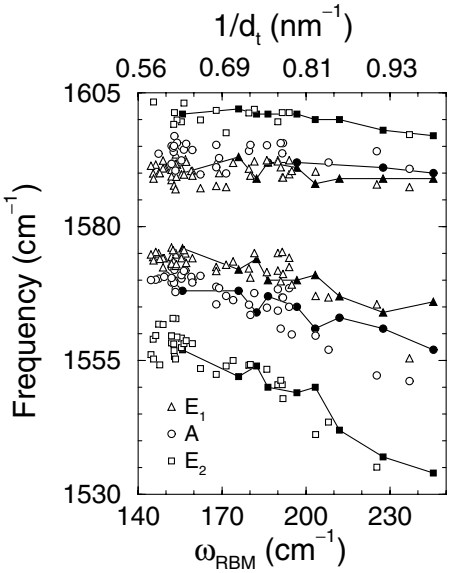

FIG. 3. ω_G (open symbols) vs ω_{RBM} (bottom axis) and $1/d_t$ (top axis) for semiconducting SWNTs. Experimental data are obtained with $E_{\mathrm{laser}} = 1.58$, 2.41, and 2.54 eV. The ω_G are clearly dependent on d_t, but there is no clear evidence for any ω_G dependence on E_{laser}. The spectra with $\omega_{\mathrm{RBM}} > 200\ \mathrm{cm}^{-1}$ were obtained with $E_{\mathrm{laser}} = 1.58$ eV. Solid symbols connected by solid lines come from *ab initio* calculations [15] downshifted by 18, 12, 12, 7, 7, 11 cm^{-1} from the bottom to the top of the *ab initio* data, respectively.

and experimental results show a stronger d_t dependence, but *ab initio* calculations seem to underestimate the G^--band mode softening for lower d_t values (mainly for the A mode). The experimental data from semiconducting SWNTs can be better fit with $\omega_G^- = 1592 - C/d_t^{\beta}$, with $\beta = 1.4$, $C_A = 41.4\ \mathrm{cm}^{-1}\,\mathrm{nm}^{1.4}$, $C_{E_1} = 32.6\ \mathrm{cm}^{-1}\,\mathrm{nm}^{1.4}$, $C_{E_2} = 64.6\ \mathrm{cm}^{-1}\,\mathrm{nm}^{1.4}$, in contrast to previous results ($\beta = 2$ [16]) obtained using only two Lorentzian peaks to fit the G-band spectra.

Finally, a polarization analysis of Raman spectra and a comparison with *ab initio* calculations are consistent with the observation of A, E_1, and E_2 symmetry modes in the G-band for SWNTs. According to the resonance Raman selection rules discussed above [13], E_2 symmetry modes can be observed only for cross polarized light (in agreement with previous work [10]) in resonance with electronic transitions from the E_μ^v to $E_{\mu\pm1}^c$ van Hove singularities. Furthermore, it is possible that only either the valence or the conduction band state will be at a van Hove singularity.

In summary, we have observed resonance Raman spectra at the single nanotube level from the same nanotube using different laser energies. The G' band exhibits a (n, m) dependent frequency dispersion with E_{laser}, in agreement with the double resonance process in 1D systems. The G-band ω_G is E_{laser} independent and can be explained by a first-order single-resonance Raman scattering process involving six ($2A$, $2E_1$, and $2E_2$) zone center modes, that can be observed by polarized Raman experiments. The d_t dependence of the six G-band modes for semiconducting SWNTs is established and the results agree quite well with *ab initio* calculations in the $1.0 < d_t < 2.0$ nm diameter range [15], thus supporting the assignment. The clear observation of E_2 modes means that resonance with $E_{\mu,\mu\pm1}$ transitions needs to be taken into account when analyzing Raman and optical absorption spectra from isolated SWNTs. This result explains previous controversial polarization studies on aligned SWNT samples, solves open questions related to the resonance nature of the G-band Raman process in SWNTs, and opens up a new perspective for the ability of optical experiments to study electronic dispersion in SWNTs. Experiments using an excitation laser with a continuously tunable energy will be important for a more detailed and quantitative study of the different $E_{\mu\mu}$ and $E_{\mu,\mu\pm1}$ resonance Raman processes in SWNTs.

The authors acknowledge helpful discussions with H. Chacham, M. S. C. Mazzoni, R. Capaz, and O. Dubay. This work is supported by CNPq/NSF joint collaboration program (NSF INT 00-00408 and CNPq 910120/99-4) and Instituto de Nanociências, Brazil. A. J. and A. G. S. F. acknowledge financial support from CNPq/CAPES-Brazil. The MIT authors acknowledge support under NSF DMR 01-16042. R. S. acknowledges a Grant-in-Aid (No. 13440091) from the Ministry of Education, Japan.

[1] G. S. Duesberg *et al.*, Phys. Rev. Lett. **85**, 5436 (2000).
[2] A. Jorio *et al.*, Phys. Rev. Lett. **86**, 1118 (2001).
[3] A. M. Rao *et al.*, Phys. Rev. Lett. **86**, 3895 (2001); Z. Yu *et al.*, J. Phys. Chem. B **105**, 1123 (2001); R. R. Bacsa *et al.*, Phys. Rev. B **65**, 161404(R) (2002); X. Zhao *et al.*, Appl. Phys. Lett. **81**, 2550 (2002).
[4] M. J. O'Connell *et al.*, Science **297**, 593 (2002).
[5] R. Saito, G. Dresselhaus, and M. S. Dresselhaus, *Physical Properties of Carbon Nanotubes* (Imperial College Press, London, 1998); M. S. Dresselhaus and P. C. Eklund, Adv. Phys. **49**, 705 (2000); M. S. Dresselhaus *et al.*, Carbon **40**, 2043 (2002), and references therein.
[6] M. A. Pimenta *et al.*, Braz. J. Phys. **30**, 423 (2000).
[7] A. G. Souza Filho *et al.*, Phys. Rev. B **65**, 035404 (2002); J. Kürti *et al.*, Phys. Rev. B **65**, 165433 (2002); J. Maultzsch *et al.*, Phys. Rev. B **64**, 121407 (2001).
[8] V. Zolyomi *et al.*, Phys. Rev. B **66**, 073418 (2002).
[9] S.-L. Zhang *et al.*, Phys. Rev. B **66**, 035413 (2002).
[10] A. Jorio *et al.*, Phys. Rev. Lett. **85**, 2617 (2000).
[11] C. Thomsen *et al.*, Phys. Status Solidi B **215**, 435 (1999).
[12] J. Maultzsch *et al.*, Phys. Rev. B **65**, 233402 (2002).
[13] M. F. Lin, Phys. Rev. B **62**, 13153 (2000); A. Grüneis *et al.*, Phys. Rev. B (to be published)
[14] J. Hwang *et al.*, Phys. Rev. B **62**, R13 310 (2000); A. Jorio *et al.*, Phys. Rev. B **65**, 121402(R) (2002).
[15] O. Dubay *et al.*, Phys. Rev. Lett. **88**, 235506 (2002).
[16] A. Jorio *et al.*, Phys. Rev. B **65**, 155412 (2002).
[17] A. Jorio *et al.*, Phys. Rev. B **66**, 115411 (2002).